Supporting Information for "Subsurface Mixing Dynamics across the Salt-freshwater Interface"

K.De Vriendt[1], T.Le Borgne[2], M.Pool[3], M.Dentz[1]

[1]IDAEA-CSIC, Institute of Environmental Assessment and Water Research, Spanish National Research Institute, Calle Jordi Girona, 18-26, 08034 Barcelona

[2]Université de Rennes 1, CNRS, Géosciences Rennes UMR 6118, Rennes, France

[3]AMPHOS 21 Consulting S. L., 08019 Barcelona

Contents of this file

1. Text S1-S4
2. Figures S1-S3
3. Table S1

Text S1: Model Parameters

Values of parameters used in the numerical simulations are provided in table S1.

Dispersivities

Numerical studies have shown that the longitudinal and transverse dispersivities α_l and α_t are important parameters when considering mixing dynamics and the width of the SFI (e.g. Abarca et al., 2007; Nick et al., 2013; Spiteri et al., 2008). Unlike the evolution of plumes over time, there exists no clear criterion for assigning the value of dispersivities (Rezaei et al., 2005). This is further confounded by the fact that it is a parameter that is generally difficult to measure and is scale dependent (Neuman, 1990). Numerical studies of field sites often adopt arbitrarily large dispersivity values in order to overcome numerical dispersion caused by poor grid refinement in numerical codes (Paster, 2010), or to artificially incorporate the effects of tides and heterogeneity (Werner et al., 2012). However, large dispersion likely lead to an overestimation of mixing induced reaction rates.

In Figure S2, we see that increasing α_l has negligible impact on the overall mixing width compared to α_t. For example, increasing α_l by a factor of 5 for $\alpha_t = 0.01$ m, results in almost no change in s_m. This is not surprising given the bulk of the interface resides where flow is tangential to the principal direction of flow. Flow from the seaside however approaches the interface orthogonally with velocities approximately an order of magnitude lower than the freshwater flux. This, however is by no means suggesting α_l play no role in the behaviour of the mixing zone. Abarca et al. (2007) showed that increasing α_l leads to the seaward displacement of high concentration isolines, with a particularly strong influence at toe. Therefore for larger values of α_l, the analytical solution may no longer provide provide a good fit. For smaller dispersivities however, which are in-line

with literature values seen in table S2, α_t alone seems to sufficiently characterizes the growth of s.

Text S2 Mixing width

To determine the mixing width, we compute the distance across $c(1-c)$ at half its maximum, denoted here as κ. Due to the proximity of the toe to boundary, the full width at half maximum cannot be attained directly at the bottom and are omitted. For a symmetric profile of $c(1-c)$, we can relate this back to the square root of the second central moment (variance) of $c(1-c)$,

$$s = \frac{\kappa}{2\sqrt{2\ln 2}}, \tag{1}$$

where s defines the mixing width.

Text S3: Interface width and interface height

We first recall that the stretching rate is defined by

$$\gamma(z) = \frac{dv(z)}{dz}. \tag{2}$$

Inserting this expression into expression (8) in the main text for $s(z)$, we can write

$$s(z) = \sqrt{\alpha_t \left[\frac{d\ln v(z)}{dz}\right]^{-1}}. \tag{3}$$

We estimate the velocity along the interface from volume conservation and set

$$v(z) = \frac{q_f b}{\xi(z)}, \tag{4}$$

where $\xi(z)$ is the interface height that is $\xi(z=0)=b$ at the toe postion at $z=0$ and 0 at the outflow. With this definition, we obtain for the interface width in Eq. (3)

$$s(z)=\sqrt{-\alpha_t\left[\frac{d\ln\xi(z)}{dz}\right]^{-1}}. \tag{5}$$

Text S4: Interface width from the Glover solution

To derive an approximation for the mixing width in the compression regime, we consider the sharp interface solution of Glover (1959) that predicts the position of the interface as,

$$\xi^2=\frac{2Q_f}{K\epsilon'}z+\frac{Q_f^2}{K^2\epsilon'^2}, \tag{6}$$

where $Q_f=q_fb$, recalling q_f is the freshwater flux and b is the domain height. To account for the influence of mixing we incorporate the empirical correction factor for the buoyancy factor, ϵ', as introduced by Pool (2011),

$$\epsilon=\epsilon'\left[1-\left(\frac{\alpha_t}{b}\right)^{1/4}\right]^{-1}. \tag{7}$$

We implement the factor 1/4 suggested by (Lu & Werner, 2013) as it provides a better fit against the numerical simulations. We transform equation (6) such that $z=0$ coincides with the toe position. Thus, we obtain

$$\xi=\sqrt{b^2-\frac{2b}{\mathsf{Ng}'}z}, \tag{8}$$

where we defined the modified gravity number, $\mathsf{Ng}'=K\epsilon/q_f$. Note that $\xi(z=0)=b$. The the length of the toe is predicted by the Glover solution as

$$L_t=\frac{b\mathsf{Ng}'}{2}. \tag{9}$$

Inserting (8) into (5), we obtain for the interface width during the compression regime the explicit expression

$$s(z) = \sqrt{\alpha_t(\mathsf{N}\mathsf{g}'b - 2z)}. \tag{10}$$

References

Abarca, E., Carrera, J., Sánchez-Vila, X., & Dentz, M. (2007). Anisotropic dispersive Henry problem. *Advances in Water Resources*, *30*(4), 913–926. doi: 10.1016/j .advwatres.2006.08.005

Abarca, E., & Clement, T. P. (2009). A novel approach for characterizing the mixing zone of a saltwater wedge. *Geophysical Research Letters*, *36*(January), 1–5. doi: 10.1029/2008GL036995

Abarca, E., Karam, H., Hemond, H. F., & Harvey, C. F. (2013). Transient groundwater dynamics in a coastal aquifer : The effects of tides , the lunar cycle , and the beach profile. *Water Resources Research*, *49*(May), 2473–2488. doi: 10.1002/wrcr.20075

Glover, R. E. (1959). The pattern of fresh-water flow in a coastal aquifer. *Journal of Geophysical Research*, *64*(4), 457–459. doi: 10.1029/jz064i004p00457

Heiss, J. W., & Michael, H. A. (2014, August). Saltwater-freshwater mixing dynamics in a sandy beach aquifer over tidal, spring-neap, and seasonal cycles. *Water Resources Research*, *50*(8), 6747–6766. Retrieved from `https://doi.org/10.1002/2014wr015574` doi: 10.1002/2014wr015574

Lu, C., & Werner, A. D. (2013). Advances in Water Resources Timescales of seawater intrusion and retreat. *Advances in Water Resources*, *59*, 39–51. Retrieved from `http://dx.doi.org/10.1016/j.advwatres.2013.05.005` doi: 10.1016/

j.advwatres.2013.05.005

Masahiro, T., Momii, K., & Luyun Jr, R. (2018). Laboratory Scale Investigation of Dispersion Effects on Saltwater Movement due to Curoff Wall Installation. In *25th salt water intrusion meeting* (pp. 323–328). Gdansk.

Neuman, P. (1990). Universal scaling of hydraulic conductivities and dispersivities in geologic media. *Water Resources Research*, *26*(8), 1749–1758.

Nick, H. M., Raoof, A., Centler, F., Thullner, M., & Regnier, P. (2013). Reactive dispersive contaminant transport in coastal aquifers : Numerical simulation of a reactive Henry problem. *Journal of Contaminant Hydrology*, *145*, 90–104. Retrieved from `http://dx.doi.org/10.1016/j.jconhyd.2012.12.005` doi: 10.1016/j.jconhyd.2012.12.005

Paster, A. (2010). Mixing between fresh and salt waters at aquifer regional scale and identification of transverse dispersivity. *Journal of Hydrology*, *380*(1-2), 36–44. Retrieved from `http://dx.doi.org/10.1016/j.jhydrol.2009.10.018` doi: 10.1016/j.jhydrol.2009.10.018

Pool, M. (2011). *Simplified approaches to deal with the complexities of Seawater Intrusion* (Unpublished doctoral dissertation).

Rezaei, M., Sanz, E., Raeisi, E., & Ayora, C. (2005). Reactive transport modeling of calcite dissolution in the fresh-salt water mixing zone. *Journal of Hydrology*, *311*, 282–298. doi: 10.1016/j.jhydrol.2004.12.017

Robinson, C., Gibbes, B., Carey, H., & Li, L. (2007). Salt-freshwater dynamics in a subterranean estuary over a spring-neap tidal cycle. *Journal of Geophysical Research*,

112(June), 1–15. doi: 10.1029/2006JC003888

Robinson, G., Hamill, G. A., & Ahmed, A. A. (2015). Automated image analysis for experimental investigations of salt water intrusion in coastal aquifers. *Journal of Hydrology*, *530*, 350–360. Retrieved from http://dx.doi.org/10.1016/j.jhydrol.2015.09.046 doi: 10.1016/j.jhydrol.2015.09.046

Spiteri, C., Slomp, C. P., Tuncay, K., & Meile, C. (2008). Modeling biogeochemical processes in subterranean estuaries : Effect of flow dynamics and redox conditions on submarine groundwater discharge of nutrients. *Water Resources Research*, *44*, 1–18. doi: 10.1029/2007WR006071

Werner, A. D., Bakker, M., Post, V. E. A., Vandenbohede, A., Lu, C., Ataie-Ashtiani, B., ... Barry, D. A. (2012). Seawater intrusion processes, investigation and management: Recent advances and future challenges. *Advances in Water Resources*. Retrieved from http://dx.doi.org/10.1016/j.advwatres.2012.03.004 doi: 10.1016/j.advwatres.2012.03.004

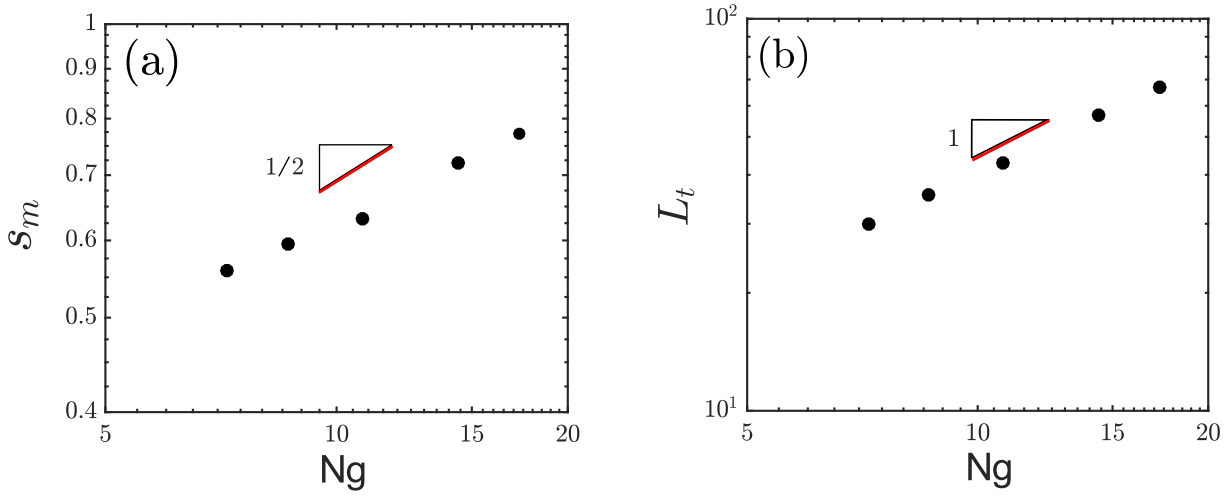

Figure S1. a) Maximum mixing width, s_m and the b) toe length, L_t obtained from numerical models as a function of Ng

Table S1. Parameters used in numerical simulations

Parameter	Value	Description
$K[ms^{-1}]$	1 x 10^{-4}	Hydraulic conductivity
$b[m]$	10	Aquifer thickness
$L[m]$	100	Aquifer Length
$\phi[-]$	0.3	Porosity
$\alpha_l[m]$	0.2	Longitudinal dispersivity
$\alpha_t[m]$	0.02	Transverse dispersivity
$q_f[md^{-1}]$	0.0125, 0.015, 0.02, 0.025 and 0.03	Freshwater flux
$\mathsf{Ng}[-]$	17.3, 14.4, 10.8, 8.6 and 7.2	Freshwater flux
D_m $[m^2/s]$	1e-9	Molecular diffusion
$\epsilon'[-]$	0.025	Buoyancy factor

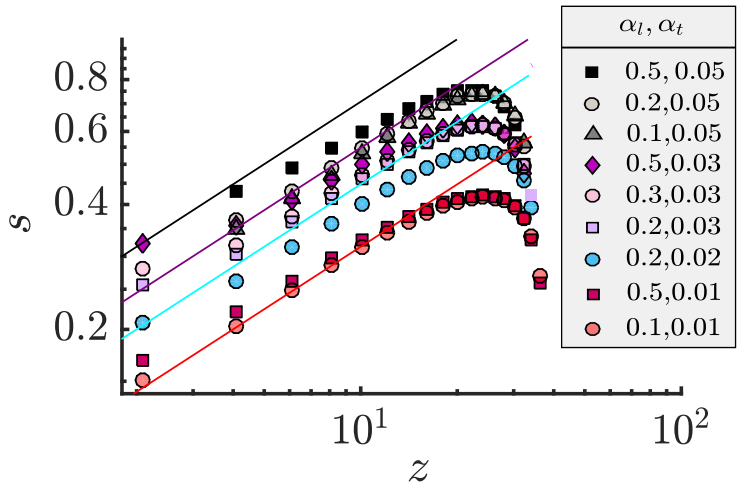

Figure S2. Mixing width for varying dispersivities. Solid lines indicate interface growth for the numerical transverse dispersivity.

Table S2. Literature derived values of coastal aquifer properties

Publication	**Type**	K [m/s]	q_f [m/d]	b [m]	α_l (m)	α_t (m)
Paster (2010)	Field	1.73×10^{-3}	-	600-1000	-	0.04
Abarca et al. (2013)	Field	1.74×10^{-4}	2.3×10^{-2}	11	0.1	0.01
Heiss and Michael (2014)	Field	2.9×10^{-4}	-	12-18	0.15	1.5×10^{-2}
Spiteri et al. (2008)	Field	6.86×10^{-4}	0.13	11	0.5	5×10^{-3}
C. Robinson et al. (2007)	Field	1.16×10^{-4}	6.6×10^{-2}	30	0.5	5×10^{-2}
Abarca and Clement (2009)	Experimental	1.2×10^{-2}	-	0.3	5×10^{-4}	5×10^{-5}
G. Robinson et al. (2015)	Experimental	2.3×10^{-3}	-	0.14	1×10^{-3}	5×10^{-4}
Masahiro et al. (2018)	Experimental	-	-	0.25	7×10^{-4}	2.5×10^{-5}

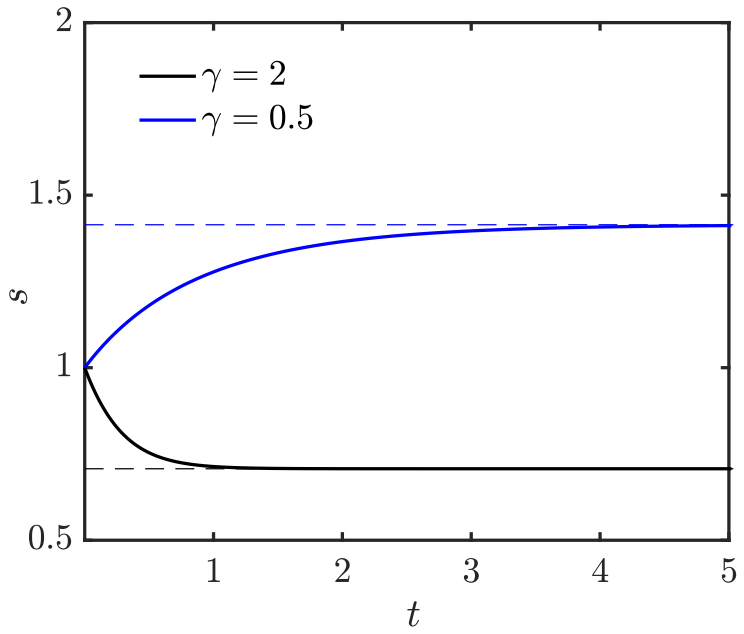

Figure S3. Evolution of mixing width given two different stretching rates. Blue line shows diffusive growth of an interface towards a large bachelor scale (blue dashed line) given a small stretching rate whereas the black line shows the mixing width compressing exponentially towards a small Batchelor scale (black dashed line)